IOPscience iopscience.iop.org

Home Search Collections Journals About Contact us My IOPscience

An environment-dependent tight-binding potential for Si

This article has been downloaded from IOPscience. Please scroll down to see the full text article.

1999 J. Phys.: Condens. Matter 11 2043

(http://iopscience.iop.org/0953-8984/11/8/017)

View the table of contents for this issue, or go to the journal homepage for more

Download details:
IP Address: 171.66.16.214
The article was downloaded on 15/05/2010 at 07:08

Please note that terms and conditions apply.

J. Phys.: Condens. Matter **11** (1999) 2043–2049. Printed in the UK PII: S0953-8984(99)97348-4

# An environment-dependent tight-binding potential for Si

C Z Wang, B C Pan and K M Ho

Ames Laboratory and Department of Physics and Astronomy, Iowa State University, Ames, IA 50011, USA

Received 9 September 1998, in final form 17 December 1998

**Abstract.** We present a new generation of tight-binding model for silicon which goes beyond the traditional two-centre approximation and allows the tight-binding parameters to scale according to the bonding environment. We show that the new model improves remarkably the accuracy and transferability of the potential for describing the structures and energies of silicon surfaces, in addition to the properties of silicon in the bulk diamond structure.

Silicon is an important material in the microelectronics industry. The structures and properties of silicon have been the subject of extensive experimental and theoretical studies over the past four decades. An outstanding problem in the computer simulation of silicon systems at the microscopic level is the need for an accurate, transferable, and yet simple model of the energetic and electronic properties of the material. *Ab initio* techniques have been well developed in the past twenty years and can provide an accurate description of the materials, but the computational cost is prohibitive for studying large systems. On the other hand, there are quite a number of empirical interatomic potentials proposed for Si [1–7]. These potentials can be used to simulate a large number of atoms, but they do not always give correct descriptions of the properties that are not explicitly included in the fitting database. There is a large class of problems which require more atoms than *ab initio* techniques can handle and demand more accuracy than classical potentials can provide.

Tight-binding molecular dynamics (TBMD) [8] bridges the gap between *ab initio* methods and classical-potential schemes. Tight-binding potentials are more accurate than classical potentials. At the same time, TBMD is much faster than *ab initio* methods because the Hamiltonian matrix elements are described by a set of parametrized functions. The scheme becomes even more attractive due to recent developments in order-$N$ algorithms for electronic calculation and the use of parallel computers [9–12]. Nevertheless, generating an accurate and transferable tight-binding potential for Si is a very challenging task due to the complicated bonding character in the material. Although an enormous effort has been devoted to developing transferable tight-binding potentials for Si in the past few years [13–18], existing tight-binding potentials are successful only in the studies of certain properties of Si, and have not always been very transferable to general geometries such as clusters and surfaces.

One of the major limitations in the transferability of previous tight-binding potentials is the assumption of two-centre approximation for the tight-binding hopping parameters [19]. For example, in silicon, each Si atom has four valence electrons which can form strong $sp^3$ hybrids in the diamond structure. In the fcc structure, however, the valence electrons are shared by twelve neighbours leading to metallic bonding. These different bonding situations

0953-8984/99/082043+07$19.50 © 1999 IOP Publishing Ltd 

suggest that the interaction strength in the diamond structure should be stronger than that in the fcc structure even when the interatomic distances are the same. It is obvious that the two-centre approximation fails to describe these different bonding situations for the two different structures. Another drawback of the two-centre approximation is that it cannot distinguish between the nearest-neighbour and further-neighbour interactions since the interaction strength depends only on the distance between the two atoms.

In this paper, we present a new generation of tight-binding potential for Si based on the environment-dependent tight-binding model that we proposed for carbon [20] which goes beyond the traditional two-centre approximation and allows the tight-binding parameters as well as the repulsive energy to be dependent on the bonding environment. We show that this new potential is very transferable and can describe well the structures and energies of silicon in many different configurations.

To make the model as simple as possible, the potential is constructed using an orthogonal $sp^3$ basis and a scaling function for the tight-binding parameters in a form similar to that in the two-centre approximation. The effects of nonorthogonality, multi-centre interactions, and the variation of the local basis set with environment are taken into account through renormalizing the pair interaction strength among atoms according to the surrounding atomic configurations.

Specifically, the hopping parameters and the pairwise repulsive potential are expressed as

$$h(r_{ij}) = \alpha_1 R_{ij}^{-\alpha_2} \exp[-\alpha_3 R_{ij}^{\alpha_4}](1 - S_{ij}). \tag{1}$$

In this expression, $h(r_{ij})$ denotes the possible types of interatomic hopping parameter $V_{ss\sigma}$, $V_{sp\sigma}$, $V_{pp\sigma}$, $V_{pp\pi}$ and pairwise repulsive potential $\phi(r_{ij})$ for atoms $i$ and $j$. $r_{ij}$ is the real distance and $R_{ij}$ is a scaled distance between atoms $i$ and $j$ (see equation (3)). $S_{ij}$ is a screening function. The parameters $\alpha_1$, $\alpha_2$, $\alpha_3$, and $\alpha_4$ and parameters for the bond-length scaling function $R_{ij}$, and the screening function $S_{ij}$ can be different for different hopping parameters and the pairwise repulsive potential. Note that expression (1) reduces to the traditional two-centre form if we set $R_{ij} = r_{ij}$ and $S_{ij} = 0$. The dependence of the tight-binding parameters on the bonding environment is introduced through the screening function $S_{ij}$ and the bond-length scaling function $R_{ij}$.

The screening function $S_{ij}$ is expressed as a hyperbolic tangent (tanh) function with argument $\xi_{ij}$ given by

$$\xi_{ij} = \beta_1 \sum_l \exp\left[-\beta_2\left(\frac{r_{il} + r_{jl}}{r_{ij}}\right)^{\beta_3}\right] \tag{2}$$

where $\beta_1$, $\beta_2$, and $\beta_3$ are adjustable parameters. The purpose of the screening function is to reduce the interaction strength between two atoms in the solid if there are intervening atoms located between them. Note that $\xi_{ij}$ depends not only on the distance between atoms $i$ and $j$, but also on the positions of the neighbours of atoms $i$ and $j$. Maximum screening effect occurs when the atom $l$ is just sitting on the line connecting the atoms $i$ and $j$ (i.e., $r_{il} + r_{lj}$ is minimum). This approach allows us to distinguish between first- and further-neighbour interactions without explicit specification of the neighbours.

The bond-length scaling function scales the distance between two atoms according to their effective coordination numbers. Longer effective bond lengths are assumed for higher coordinated atom pairs. The strength of the parameters for hopping between atoms $i$ and $j$ are therefore dependent on the coordination number of the atoms: weaker interaction strength for higher-coordinated structures. The scaling between the real and effective interatomic distance is given by

$$R_{ij} = r_{ij}(1 + \delta_1\Delta + \delta_2\Delta^2 + \delta_3\Delta^3) \tag{3}$$

where

$$\Delta = \frac{1}{2}\left[\left(\frac{n_i - n_0}{n_0}\right) + \left(\frac{n_j - n_0}{n_0}\right)\right] \quad (4)$$

is the fractional coordination number relative to the coordination number of the diamond structure $n_0$, averaging between the coordination numbers $n_i$ and $n_j$ of atoms $i$ and $j$. The coordination number is calculated as a smooth function, $n_i = \sum_j (1 - S_{ij})$, where $S_{ij}$ has the form of the screening function described above. Note that when $i$ and $j$ are nearest-neighbour atoms, $S_{ij}$ is close to 0 and $n_i$ counts almost one neighbour. Otherwise, $S_{ij}$ is close to one if $i$ and $j$ are not nearest-neighbour atoms, and $n_i$ counts only a small fraction of a neighbour. By choosing the parameters for $S_{ij}$ as $\beta_1 = 2.0$, $\beta_2 = 0.028\,95$, and $\beta_3 = 7.962\,84$, $n_i$ is calculated to be 2.08, 3.14, 4.31, 6.14, 7.23, 10.00, and 11.93 for the linear-chain, graphite, diamond, simple-cubic, $\beta$-tin, bcc, and fcc structures respectively. These values give a reasonable representation of the effective coordination of these structures.

Besides the hopping parameters, the diagonal matrix elements are also dependent on the bonding environments. The expression for the diagonal matrix elements is

$$e_{\lambda,i} = e_{\lambda,0} + \sum_j \Delta e_\lambda(r_{ij}) \quad (5)$$

where the expression for $\Delta e_\lambda(r_{ij})$ takes the same form as equation (1), and $\lambda$ denotes the two types of orbital (s or p). $e_{s,0}$ and $e_{p,0}$ are chosen to be $-2.924\,75$ eV and $3.857\,95$ eV respectively.

Finally, we express the repulsive energy term in a functional form as in the previous tight-binding model for carbon developed by Xu *et al* [21]; that is,

$$E_{rep} = \sum_i f\left(\sum_j \phi(r_{ij})\right) \quad (6)$$

where $\phi(r_{ij})$ is a pairwise potential for atoms $i$ and $j$, and $f$ is a functional expressed as a fourth-order polynomial with argument $x = \sum_j \phi(r_{ij})$, i.e.,

$$f(x) = \sum_{n=0}^{n=4} c_n x^n. \quad (7)$$

**Table 1.** The parameters obtained from the fitting. $\alpha_1$ is in eV. The other parameters are dimensionless.

| | $\alpha_1$ | $\alpha_2$ | $\alpha_3$ | $\alpha_4$ | $\beta_1$ | $\beta_2$ | $\beta_3$ |
|---|---|---|---|---|---|---|---|
| $V_{ss\sigma}$ | −5.9974 | 0.4612 | 0.1040 | 2.3000 | 4.4864 | 0.1213 | 6.0817 |
| $V_{sp\sigma}$ | 3.4834 | 0.0082 | 0.1146 | 1.8042 | 2.4750 | 0.1213 | 6.0817 |
| $V_{pp\sigma}$ | 11.1023 | 0.7984 | 0.1800 | 1.4500 | 1.1360 | 0.1213 | 6.0817 |
| $V_{pp\pi}$ | −3.6014 | 1.3400 | 0.0500 | 2.2220 | 0.1000 | 0.1213 | 6.0817 |
| $\phi$ | 126.640 | 5.3600 | 0.7641 | 0.4536 | 37.00 | 0.56995 | 19.30 |
| $\Delta e_s$, $\Delta e_p$ | 0.2830 | 0.1601 | 0.050686 | 2.1293 | 7.3076 | 0.07967 | 7.1364 |
| | $\delta_1$ | $\delta_2$ | $\delta_3$ | | | | |
| $V_{ss\sigma}$ | 0.0891 | 0.0494 | −0.0252 | | | | |
| $V_{sp\sigma}$ | 0.1735 | 0.0494 | −0.0252 | | | | |
| $V_{pp\sigma}$ | 0.0609 | 0.0494 | −0.0252 | | | | |
| $V_{pp\pi}$ | 0.4671 | 0.0494 | −0.0252 | | | | |
| $\phi$ | 0.082661 | −0.023572 | 0.006036 | | | | |
| $\Delta e_s$, $\Delta e_p$ | 0.7338 | −0.03953 | −0.062172 | | | | |

**Table 2.** The coefficients of the polynomial function $f(x)$.

| | $c_0$ (eV) | $c_1$ | $c_2$ (eV$^{-1}$) | $c_3$ (eV$^{-2}$) | $c_4$ (eV$^{-3}$) |
|---|---|---|---|---|---|
| $x \geqslant 0.7$ | $-0.739 \times 10^{-6}$ | 0.96411 | 0.68061 | −0.20893 | 0.02183 |
| $x < 0.7$ | −1.8664 | 6.3841 | −3.3888 | 0.0 | 0.0 |

The parameters in the model are determined by first fitting to the self-consistent first-principles density functional calculation results for electronic band structures, and then the cohesive energy versus volume curves of diamond, $\beta$-tin, simple cubic, bcc, and fcc structures respectively. Additional checks have also been made to ensure that the model gives reasonable results for the elastic constants and phonon frequencies in the diamond structure. The parameters obtained from such fittings are listed in tables 1 and 2. The cut-off distance for the interactions is chosen to be 5.2 Å. The choice of the cut-off distance is somewhat arbitrary. It makes the TB model reasonably short ranged. This cut-off distance is chosen before fitting the TB parameters; it is therefore consistent with the resulting TB parameters.

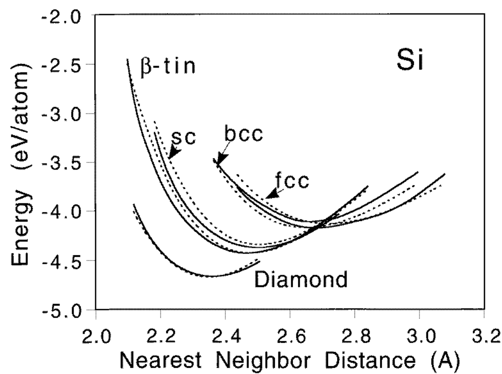


**Figure 1.** The cohesive energies as a function of nearest-neighbour distance for silicon in different crystalline structures calculated using the present TB model are compared with the results from the first-principles LDA calculations. The solid curves are the TB results and the dashed curves are the LDA results.

The cohesive energies as a function of nearest-neighbour distance for silicon in different crystalline structures obtained from the present tight-binding potential are in good agreement with the first-principles calculation results as one can see from figure 1. The potential also describes reasonably well the phonon frequencies and elastic constants of the diamond structure. The vibration frequencies at the zone centre (LTO($\Gamma$)) and at the zone boundary (TO(X), TA(X), and LOA(X)) calculated from this potential are 16.2, 12.8, 5.0, and 11.5 THz in comparison with experimental values of 15.53, 13.90, 4.49, and 12.32 THz respectively. The elastic constants $c_{11} - c_{12}$ and $c_{44}$ obtained from this potential are $0.993 \times 10^{12}$ erg cm$^{-3}$ and $0.716 \times 10^{12}$ erg cm$^{-3}$ respectively in comparison with experimental results of $1.012 \times 10^{12}$ erg cm$^{-3}$ and $0.796 \times 10^{12}$ erg cm$^{-3}$. The lattice constant and bulk modulus of the diamond structure, from this potential, are 5.45 Å and $0.90 \times 10^{12}$ erg cm$^{-3}$, which are also in good agreement with the experimental values of 5.43 Å and $0.978 \times 10^{12}$ erg cm$^{-3}$ respectively. The potential has also been applied successfully in studying the structures of silicon clusters [22] and silicon grain boundaries [23].

To further assess the transferability of the potential as regards describing more complex

structures that are not present in the fitting database, we have applied the potential to study point defects in bulk silicon and the surface reconstructions of the silicon (100) and (111) surfaces. In these calculations, a Hubbard-like on-site term

$$H_u = \frac{u}{2}(q_i - q_0)^2 \tag{8}$$

where $q_i$ is the Mulliken charge of atom $i$ and $q_0$ is equal to 4 for each silicon atom, is incorporated into the tight-binding Hamiltonian to deal with the charge transfer in these systems. The parameter $u$ is chosen to be 4 eV in our present calculations, which gives reasonable charge transfer on the silicon surfaces.

The point defect calculations are performed using a supercell of 215 atoms for vacancies and 217 atoms for self-interstitials. The tetrahedral (T), hexagonal (H), and the [110]-split (S) interstitial configurations are studied. The defect structures are fully relaxed until the largest force on a single atom is less than 0.02 eV Å$^{-1}$. The formation energies calculated after the relaxation are 3.83, 3.60, 3.65, and 3.32 eV respectively for the vacancy and the T, H, and S interstitials. Note that the present tight-binding calculation predicts that the [110]-split interstitial is the lowest-energy configuration for a self-interstitial in Si, in very good agreement with *ab initio* calculation [24].

Predicting the structures and the energies of the silicon surface reconstructions provides a big challenge for the present tight-binding potential, as all the previous tight-binding potentials fail to describe the reconstructions of the Si(100) and Si(111) surfaces correctly [18, 25]. Our structural optimizations of the Si(100) and Si(111) surfaces are performed with a slab of 12 layers (including the adatom layers for the Si(111)–(7 × 7) structure). Supercells containing 342 to 498 atoms are used in the calculations. For each reconstructed structure, all of the atoms in the slab are allowed to be relaxed until the largest force on an atom is less than 0.01 eV Å$^{-1}$.

**Table 3.** Surface energies of the silicon (100) and (111) surfaces. $\Delta E$ is the energy relative to that of the ideal (1 × 1) surface. The energies are in units of eV per (1 × 1) surface area.

| Structure | Surface energy | $\Delta E$ |
|---|---|---|
| Si(100) | | |
| (1 × 1), ideal | 2.292 | 0.0 |
| (2 × 1) | 1.153 | −1.139 |
| p(2 × 2) | 1.143 | −1.149 |
| c(4 × 2) | 1.148 | −1.144 |
| Si(111) | | |
| (1 × 1), ideal | 1.458 | 0.0 |
| (1 × 1), relaxed | 1.435 | −0.025 |
| (1 × 1), faulted | 1.495 | 0.037 |
| ($\sqrt{3} \times \sqrt{3}$)–$t_4$ | 1.213 | −0.245 |
| ($\sqrt{3} \times \sqrt{3}$)–$h_3$ | 1.346 | −0.112 |
| (2 × 1), Haneman | 1.188 | −0.270 |
| (2 × 1), $\pi$-bonded chain | 1.138 | −0.320 |
| (7 × 7), DAS | 1.099 | −0.359 |

For the Si(100) surface, we have optimized the (2 × 1), c(4 × 2), and p(2 × 2) reconstructed structures. The surface energies of the various reconstructed structures obtained from the present tight-binding model are listed in table 3. We find that the surface energy gains about 1.14 eV per (1 × 1) surface area upon reconstruction. The p(2 × 2) and c(4 × 2) reconstructions have energies slightly lower than that of the (2 × 1) reconstruction. Most notably, the present tight-binding potential correctly predicts the asymmetric dimer buckling structure

for the reconstruction. The buckling angle is 18.3° for the (2 × 1) reconstruction and slightly larger for the p(2 × 2) and c(4 × 2) reconstructions. This is in excellent agreement with the most recent LDA calculation result of 19° [26].

For the Si(111) surface, we have studied the structures and energies of the (2×1) $\pi$-bonded chain model [27], the (2 × 1) Haneman model [28], the (7 × 7) dimer–adatom–stacking-fault (DAS) model [29], and the $(\sqrt{3} \times \sqrt{3})$–$t_4$, and the $(\sqrt{3} \times \sqrt{3})$–$h_3$ structures. The surface energies obtained from our present calculations are also listed in table 3. The energy orderings of the different structures are in very good agreement with LDA calculations [30, 31] and experimental observations. In particular, the lowest-energy structure is found to be the (7 × 7) DAS reconstructed structure. Large buckling (with a buckling angle of 14.7°) is also found for the (2 × 1) $\pi$-bonded reconstructed surface. We also calculated the energy of the Si(111)–(1 × 1) stacking-fault structure, which is found to be 0.06 eV per (1 × 1) surface area higher than that of the relaxed (1 × 1) structure. This result is also in excellent agreement with the LDA calculation result [30].

In summary, we present a new generation of tight-binding model for Si which goes beyond the traditional two-centre approximation and allows the tight-binding parameters to scale according to the bonding environment. We show that the new model improves remarkably the transferability of the potential for describing the structures and energies of defects and surfaces. We anticipate that the potential will be useful for molecular dynamics simulation studies of temperature-dependent properties of silicon-based materials.

## Acknowledgments

Ames Laboratory is operated for the US Department of Energy by Iowa State University under contract No W-7405-Eng-82. This work was supported by the Director for Energy Research, Office of Basic Energy Sciences, and the High Performance Computing and Communications initiative, including a grant of computer time at the National Energy Research Supercomputing Center.

## References

[1] Stillinger F H and Weber T A 1985 *Phys. Rev.* B **31** 5262
[2] Tersoff J 1986 *Phys. Rev. Lett.* **56** 632
Tersoff J 1988 *Phys. Rev.* B **37** 6991
[3] Biswas R and Hamann D R 1985 *Phys. Rev. Lett.* **55** 2001
[4] Dodson B W 1987 *Phys. Rev.* B **35** 2795
[5] Chelikowsky J R, Phillips J C, Kamal M and Strauss M 1989 *Phys. Rev. Lett.* **62** 292
[6] Baskes M I 1987 *Phys. Rev. Lett.* **59** 2666
[7] Khor K E and Das Sarma 1988 *Phys. Rev.* B **38** 3318
[8] Wang C Z and Ho K M 1996 *Adv. Chem. Phys.* **93** 651
[9] Li X-P, Nunes R W and Vanderbilt D 1993 *Phys. Rev.* B **47** 10 891
[10] Daw M S 1993 *Phys. Rev.* B **47** 10 895
[11] Mauri F, Galli G and Car R 1993 *Phys. Rev.* B **47** 9973
[12] Qiu S Y, Wang C Z, Ho K M and Chan C T 1994 *J. Phys.: Condens. Matter* **6** 9153
[13] Goodwin L, Skinner A J and Pettifor D G 1989 *Europhys. Lett.* **9** 701
[14] Sawada S 1990 *Vacuum* **41** 612
[15] Kohyama M 1991 *J. Phys.: Condens. Matter* **3** 2193
[16] Kwon I, Biswas R, Wang C Z, Ho K M and Soukoulis C M 1994 *Phys. Rev.* B **49** 7242
[17] Mercer J L Jr and Chou M Y 1993 *Phys. Rev.* B **47** 9366
Mercer J L Jr and Chou M Y 1994 *Phys. Rev.* B **49** 8506
[18] Stokbro K, Chetty N, Jacobsen K W and Norskov J K 1994 *Phys. Rev.* B **50** 10 727
Stokbro K 1994 *PhD Thesis* Danish Technical University, Lyngby

[19] Slater J C and Koster G F 1954 *Phys. Rev.* **94** 1498
[20] Tang M S, Wang C Z, Chan C T and Ho K M 1996 *Phys. Rev.* B **53** 979
[21] Xu C H, Wang C Z, Chan C T and Ho K M 1992 *J. Phys.: Condens. Matter* **4** 6047
[22] Ho K M, Shvartsburg A A, Pan B C, Lu Z Y, Wang C Z, Wacker J G, Fye J L and Jarrold M F 1998 *Nature* **392** 582
[23] Morris J R, Lu Z Y, Ring D M, Xing J B, Ho K M and Wang C Z 1998 *Phys. Rev.* B **58** 11 241
[24] Zhu J, Diaz de la Rubia T, Yang L H, Mailhiot Ch and Gilmer G 1996 *Phys. Rev.* B **54** 4741
[25] Mercer J L Jr and Chou M Y 1993 *Phys. Rev.* B **48** 5374
[26] Kruger P and Pollmann J 1995 *Phys. Rev. Lett.* **74** 1155
[27] Pandey K C 1981 *Phys. Rev. Lett.* **47** 1913
[28] Haneman D 1961 *Phys. Rev.* **121** 1093
[29] Takayanagi K, Tanishiro Y, Takahashi M and Takahashi S 1985 *J. Vac. Sci. Technol.* A **3** 1502
[30] Vanderbilt D 1987 *Phys. Rev. Lett.* **59** 1456
[31] Northrup J E 1986 *Phys. Rev. Lett.* **57** 154